JOURNAL OF CATALYSIS 145, 508–515 (1994)

Kinetics of CO Oxidation on Cu/Rh(100) Model Bimetallic Catalysts

Janos Szanyi[1] and D. Wayne Goodman[2]

Department of Chemistry, Texas A&M University, College Station, Texas 77843-3255

Received April 16, 1993; revised September 20, 1993

The oxidation of carbon monoxide has been studied on a series of Cu/Rh(100) model bimetallic catalysts using a combined elevated pressure reactor–ultrahigh vacuum surface analysis system. The effects of temperature and oxygen/carbon monoxide partial pressures on the rates of CO_2 formation and surface composition/morphology were determined. Although the addition of copper to Rh(100) altered the rate of CO oxidation, the kinetic behavior of the Cu/Rh(100) catalysts was essentially the same as that for Rh(100) with modifications within the low Cu coverage region, i.e., at $\theta_{Cu} < 0.5$ ML. The altered kinetics are attributed to two types of reaction sites at these low Cu coverages. The primary role of copper in the Cu/Rh(100) bimetallic catalyst is to increase the surface oxygen coverage. The presence of Cu and Rh carbonate-like surface species was evident in postreaction TPD analysis.

INTRODUCTION

The removal of CO from automotive exhaust and factory effluent gas streams is a major environmental concern. The catalytic oxidation of CO on noble metals Pt, Pd, and Rh has long been utilized in catalytic converters. On the other hand, the relative simplicity of CO oxidation makes this reaction ideal to study the basic phenomena that are vital in heterogeneous catalytic processes. The CO–O_2 reaction has been extensively studied on both supported (1–5) and model single-crystal catalysts of Pt (6–8), Pd (8), Rh (9–13), Ir (8), and Ru (11, 14, 15). Kinetic and mechanistic studies (6, 8–10, 13) suggest that the reaction on these transition metal surfaces follows a Langmuir–Hinshelwood mechanism, that is, the reaction proceeds by the combination of dissociatively adsorbed oxygen [O(a)] and adsorbed CO [CO(a)]. Under most of the reaction conditions studied, the metal surfaces are predominantly covered by CO and the rate-determining step is the desorption of CO. O_2 adsorbs dissociatively on the available sites. The reaction between O(a) and CO(a) is fast and the CO_2 desorbs as it is formed.

The adsorption–desorption of CO, O_2, and CO_2 as well as the interaction among the adsorbed species on both polycrystalline and single-crystal Rh surfaces have been studied extensively (16). CO desorbs from Rh(100) at a maximum peak temperature of 490 K (17), suggesting that the surface at elevated pressures is covered exclusively by CO(a) at low temperatures (<600 K). At 500 K and at a CO pressure of 8 Torr (1 Torr = 133.32 Pa), the reaction has been shown to be first order in oxygen pressure up to O_2/CO = 13 (10). At higher oxygen pressures the reaction rate rolls over and becomes negative order in oxygen. In this region, due to the high oxygen pressure, the surface becomes oxidized, verified by postreaction Auger surface analysis (10). The sudden increase in the O/Rh Auger ratio coincides with the roll over of the reaction rate. The rates of CO oxidation on these oxygen-covered surfaces are much lower than that on metallic Rh. Under strongly oxidizing conditions the surface, in addition to being oxidized, is also covered with a carbonate-like surface species. Under these conditions, the reaction is limited by the decomposition of surface carbonate (18, 19).

The relatively strong adsorption of CO on Rh results in a negative first order CO pressure dependence with respect to CO oxidation over a wide range of temperatures and CO pressures. At a CO/O_2 ratio of 1 and a total pressure of 16 Torr, the apparent activation energy was found to be about 105 kJ/mol for Rh(100) and Rh(111) (10), in good agreement with the value 126 kJ/mol found for a supported 0.01% Rh/Al_2O_3 catalyst (20). The apparent activation energy is significantly different from this value at low temperatures (<450 K) or at high CO/O_2 (>5) ratios. Under these conditions the apparent activation energy is strongly affected by the heat of CO desorption which, in turn, is CO-coverage dependent (21). The higher the CO coverage for a given set of reaction conditions, the lower the heat of adsorption and consequently the lower the apparent activation energy. Under highly oxidizing conditions the apparent activation energy is influenced by the energy of decomposition of a surface carbonate species (18).

It has long been known that additives can significantly alter the adsorption and catalytic properties of metal cata-

[1] Present address: Los Alamos National Laboratory, CLS-1, MSJ565, Los Alamos, NM 87545.

[2] To whom correspondence should be addressed.

0021-9517/94 $6.00

lysts (30). In bimetallic catalysts the addition of a second metal to a transition metal catalyst can largely affect its activity, selectivity and resistance toward poisoning (22, 23, 31). To a large extent the altered properties of these bimetallic systems can be related to electronic interactions between the two metals (24). For example, copper was found to promote the dehydrogenation of cyclohexane to benzene on Ru(0001) by approximately an order of magnitude at a Cu coverage of ~0.7 ML (23). Furthermore, the desorption temperature of CO from $Cu_{1.0\ ML}$/Rh(100) is shifted toward higher temperatures compared to that of bulk Cu (17). Bimetallic Cu/Rh(100) catalysts were found to have enhanced activities for CO oxidation compared to either Rh(100) or Cu(100) (25). Silica-supported Cu/Pd bimetallic catalysts exhibit higher CO oxidation activities than either of the monometallic systems (26).

In this paper we report results on the kinetics of CO oxidation on Cu/Rh(100) bimetallic catalysts in the Cu coverage range 0–3 ML. The goal of this study was to explore the effects of Cu deposition by comparing the results obtained on Cu/Rh(100) systems with those measured on clean Rh(100).

EXPERIMENTAL

The experiments were carried out in a combined elevated pressure reactor–ultrahigh vacuum (UHV) surface analysis system which is described in detail elsewhere (27). The UHV surface analytical chamber, with a base pressure of $<3 \times 10^{-10}$ Torr, is equipped with Auger electron spectroscopy (AES), temperature-programmed desorption (TPD), ion sputtering, and gas- and metal dosing capabilities. The sample preparation and surface characterization were carried out in the UHV chamber. The Rh(100) crystal was heated resistively by a tantalum wire spotwelded to the back face of the sample. The sample temperature was monitored using a W–5%Re/W–26%Re thermocouple spotwelded to the edge of the crystal. Repeated cycles of oxidation in 10^{-7} Torr of oxygen at 800 K followed by annealing at 1200 K in UHV for 2 min were used to clean the Rh(100) crystal. Cu was deposited onto the clean Rh(100) surface at a substrate temperature of 300 K from an oxygen-free Cu wire wrapped around a tungsten filament. The cleanliness of the Rh(100) crystal and the amount of Cu deposited were monitored by AES. The amount of deposited Cu was determined using a calibration curve of Cu/Rh Auger ratio versus Cu TPD peak area (17). Following surface characterization, the sample was transferred into the elevated pressure reaction chamber through doubly differentially pumped teflon sliding seals. The reaction chamber is connected to a gas handling system and a gas chromatograph (GC) equipped with a flame ionization detector (FID).

Upon completion of a catalytic experiment the reactant–product gas mixture was pumped through a liquid-nitrogen-cooled sample loop to quantitatively trap the CO_2 product. CO_2 was introduced onto the GC column by warming the trap to ~350 K. Following separation, the CO_2 was passed over a methanizer and converted quantitatively to CH_4, which in turn, was analyzed via a flame ionization detector (FID).

Research purity (>99.999%, Matheson) CO and O_2 were utilized. CO was further purified by passing it through a 142-K *n*-pentane/liquid-nitrogen slurry trap in order to remove transition metal (Fe,Ni)-carbonyl impurities. Oxygen was used as received. CO/O_2 reactant mixtures with varying ratios were prepared and stored in glass bottles for a minimum of 12 h to assure complete mixing. In the partial pressure dependence studies, CO and O_2 were mixed *in situ* in the reaction cell. Following the catalytic experiments the sample was transferred into the UHV chamber where surface analysis was carried out by AES. Postreaction TPD experiments were also carried out to monitor the decomposition of any surface species.

RESULTS

1. The Effect of Reaction Temperature

The effect of temperature on the rate of CO oxidation was studied on a series of Cu/Rh(100) catalysts with Cu coverages of 0.0, 0.8, 1.0, and 1.3 ML in the temperature range $390 < T < 460$ K using a $CO/O_2 = 2$ reactant gas mixture. The results obtained are shown in Fig. 1 in Arrhenius form. The apparent activation energy for Rh(100) was found to be 101 ± 2 kJ/mol, in agreement with previous literature values (9, 10). The activation energy was essentially the same for all three Cu/Rh(100) samples, 108 ± 4 kJ/mol.

2. Oxygen Partial Pressure Dependence

a. The effect of oxygen pressure on the catalytic activity. The dependence of the turnover frequency (TOF) for CO_2 production on the oxygen pressure was investigated at 500 K and a constant CO pressure of 8 Torr on a series of Cu/Rh(100) catalysts with Cu coverages of 0.00, 0.25, 0.60, 1.1, and 1.75 ML. The oxygen pressure dependencies are shown in Fig. 2. A positive first-order oxygen pressure dependence was seen for the clean Rh(100) sample in the range of $0.5 < P_{O_2} < 75$ Torr. A rollover region between 75 and 100 Torr was observed within which the positive first order changes to negative 0.5. On Rh(100) this rollover region is very narrow; the change from 1.0 to −0.5 order takes place in a very small oxygen pressure interval. The deposition of about a quarter of a monolayer Cu on the Rh(100) surface resulted in an enhanced CO_2 production rate compared to the clean

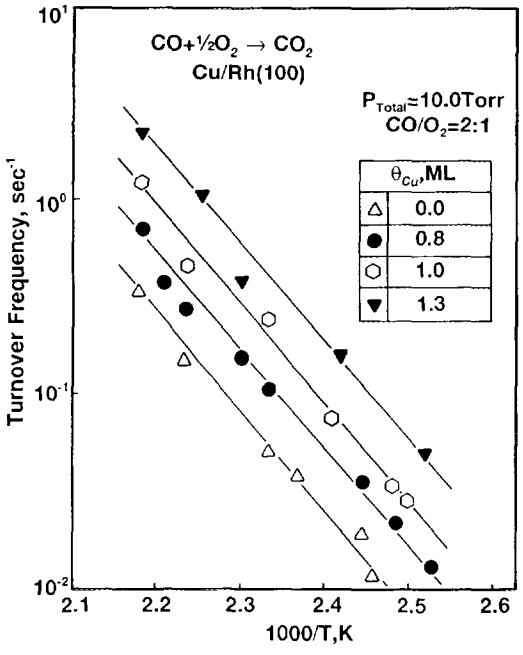

FIG. 1. Arrhenius plots for CO oxidation on various Cu/Rh(100) catalysts. P_{Total} = 10 Torr; CO/O_2 = 2/1.

Rh(100). At the same time, the order of the reaction with respect to oxygen fell significantly below 1.0. The positive first-order O_2 pressure dependence observed for copper-free Rh(100) decreases to ±0.6 for $Cu_{0.25}$/Rh(100) in the $0.5 < P_{O_2} < 50$ Torr range. Furthermore the catalyst reached its maximum activity at ~50 Torr oxygen compared to ~75 Torr for Rh(100). The activity of this $Cu_{0.25\ ML}$/Rh(100) catalyst, unlike the copper-free Rh(100), does not roll over in a very narrow P_{O_2} range but rather exhibits almost zero-order behavior over a wide pressure window ($50 < P_{O_2} < 200$ Torr). Increasing the amount of Cu deposited to 0.6 ML results in catalytic properties characteristic of both the copper-free Rh(100) and the $Cu_{0.25\ ML}$/Rh(100) catalysts.

The activity of $Cu_{0.60\ ML}$/Rh(100) is higher than that for the copper-free Rh(100). However, for $Cu_{0.60}$/Rh(100) the O_2 pressure dependence in the range $0 < P_{O_2} < 50$ Torr was essentially identical to that observed for copper-free Rh(100), that is, approximately positive first order. There is an extended oxygen pressure range from 50 to 250 Torr within which the reaction was zero order in P_{O_2}. At $P_{O_2} > 250$ Torr the reaction rate became negative order in P_{O_2}.

The $Cu_{1.1\ ML}$/Rh(100) catalyst showed behavior very similar to the $Cu_{0.60\ ML}$/Rh(100) sample. The initial positive order in oxygen pressure becomes zero order at ~50 Torr oxygen. The reaction rate in oxygen pressure becomes negative order above 250 Torr. However the $Cu_{1.1}$/Rh(100) catalyst exhibited a lower catalytic activity in the P_{O_2} range 0.0–50 Torr than did the $Cu_{0.60\ ML}$/Rh(100).

A somewhat different catalytic behavior was seen for the $Cu_{1.75\ ML}$/Rh(100) sample. At low oxygen pressures ($P_{O_2} < 2$ Torr) the catalyst was much less active toward CO oxidation compared to the lower Cu coverages. The TOFs for $Cu_{1.75\ ML}$/Rh(100) in this oxygen pressure range were close to those seen for Rh(100). At P_{O_2} = 5 Torr the activity increased markedly to the values found for Cu coverages ≤1.1 ML. For oxygen partial pressures >5 Torr, the catalyst exhibited the same behavior as those catalysts with Cu coverages >0.5 ML.

b. The effect of oxygen pressure on the surface composition and morphology. The changes in surface composition and morphology were followed by postreaction Auger analysis and, in certain cases, with TPD. The samples were flashed to reaction temperature in UHV prior to Auger analysis to remove adsorbed CO and O_2. In Figs. 3 and 4 the Cu/Rh and O/Rh Auger ratios, respectively, are displayed as a function of the oxygen pressure. On the $Cu_{0.25\ ML}$/Rh(100) catalyst the Cu overlayer was stable over the entire oxygen pressure range studied, indicated by the constant Cu/Rh Auger ratios in Fig. 3. The oxygen coverage on the $Cu_{0.25\ ML}$/Rh(100) catalyst is stable and low within the range of oxygen pressures between 0.5 and 150 Torr (see Fig. 4). At $P_{O_2} > 150$ Torr the Cu/Rh ratio increased monotonically with increasing P_{O_2} and ultimately became larger than the original Cu/Rh ratio at high oxygen pressures (>250 Torr). The Cu overlayer on the $Cu_{1.1\ ML}$/Rh(100) sample was stable in the low oxygen

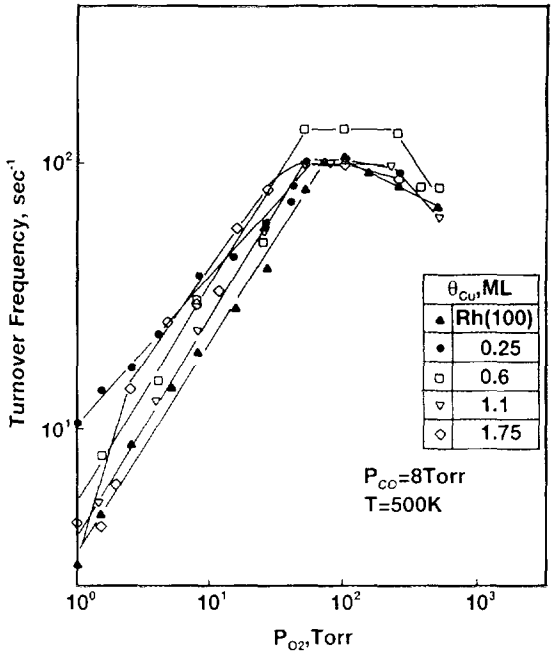

FIG. 2. CO_2 formation rates for various Cu/Rh(100) catalysts as a function of O_2 partial pressure. P_{CO} = 8 Torr; T = 500 K.

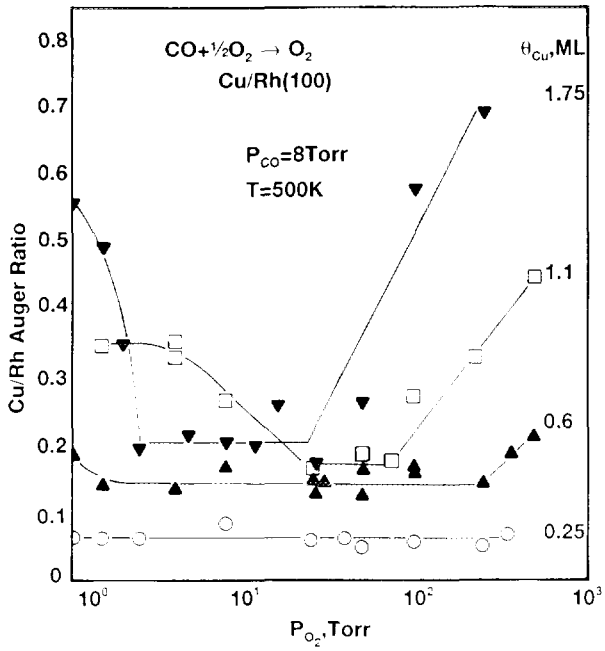

FIG. 3. Post-reaction Cu/Rh Auger ratios for various Cu/Rh(100) catalysts after reaction as a function of O_2 partial pressure. P_{CO} = 8 Torr; T = 500 K.

pressure range 0.5–4.0 Torr then decreased linearly as the oxygen pressure increased from 4 to 15 Torr. In this P_{O_2} range the Cu/Rh Auger ratio dropped from the initial value of 0.36 to 0.18 and then stayed constant in the range $15 \leq P_{O_2} < 80$ Torr. A further increase in the oxygen pressure resulted in an increase in the Cu/Rh Auger ratio; at $P_{O_2} > 200$ Torr the Cu/Rh Auger ratio exceeded the initial value of 0.36. The oxygen pressure at the onset of the increase in the Cu/Rh ratio is much lower for $Cu_{1.1\ ML}$/Rh(100) than for the $Cu_{0.6\ ML}$/Rh(100), namely 80 Torr compared to 150 Torr. There is a very sharp decrease in the Cu/Rh Auger ratio for the $Cu_{1.75\ ML}$/Rh(100) sample in the oxygen pressure range 0.5–4.0 Torr. The Cu/Rh Auger ratio, after dropping from the initial value of 0.56 to 0.21 at 4.0 Torr, remained constant up to 50 Torr oxygen. Beginning at $P_{O_2} \approx 50$ Torr the Cu/Rh ratio increased linearly with increasing oxygen pressure. The Cu/Rh Auger ratio reached a stable value at a significantly lower oxygen pressure for $Cu_{1.75\ ML}$/Rh(100) than for $Cu_{1.1\ ML}$/Rh(100) (4 Torr vs 80 Torr, respectively). At intermediate oxygen pressure (~10 Torr) the Cu/Rh Auger ratios for initial Cu coverages of 1.75 and 1.1 were essentially the same.

In agreement with earlier studies (10) postreaction Auger analysis showed essentially zero residual oxygen on the Rh(100) surface at oxygen pressures less than 170 Torr (see Fig. 4). At an oxygen pressure corresponding to the maximum activity (~85 Torr) on Rh(100) the onset of oxidation was apparent with the O/Rh Auger ratio increasing monotonically with increasing oxygen pressure. The $Cu_{0.25\ ML}$/Rh(100) exhibited a very similar behavior; however, a low level, stable oxygen coverage was apparent on this surface up to an oxygen pressure of ~40 Torr. Above 40 Torr, the O/Rh ratio increased more dramatically than for the Cu-free Rh(100). A somewhat higher coverage of oxygen was present on the $Cu_{0.60\ ML}$/Rh(100) surface even at 2 Torr and remained constant up to oxygen pressures of ~40 Torr. At $P_{O_2} > 40$ Torr, the oxygen coverage increased markedly. The $Cu_{1.1\ ML}$/Rh(100) and $Cu_{1.75\ ML}$/Rh(100) systems exhibited an initial decrease in the O/Rh Auger ratio, a stable oxygen level in the $4 < P_{O_2} < 40$ Torr range, followed by a sharp increase in the O/Rh AES ratio.

The formation of a carbonate species on Rh during CO oxidation has been suggested previously (18, 19). In postreaction TPD, CO_2 desorbs from Rh(111) at a desorption peak temperature of 550 K (19). The formation of a surface carbonate during CO oxidation has also been observed on a Cu(100) surface (29). In postreaction TPD CO_2 desorbed at a peak temperature of about 630 K from the Cu(100) surface. Following CO oxidation on Rh(100)

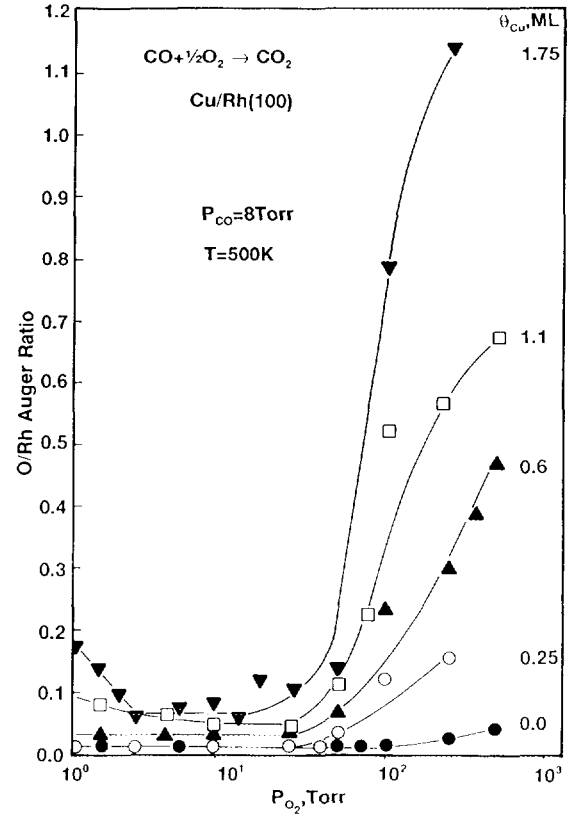

FIG. 4. Post-reaction O/Rh Auger ratios for various Cu/Rh(100) catalysts after reaction as a function of O_2 partial pressure. P_{CO} = 8 Torr; T = 500 K.

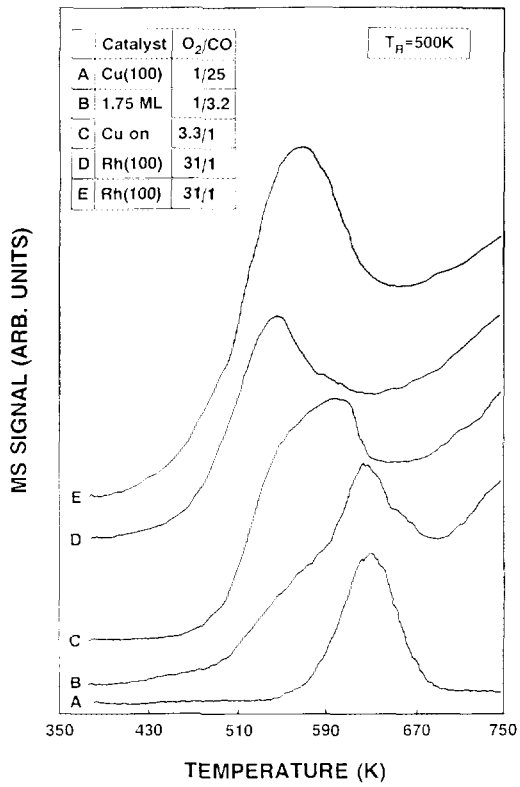

FIG. 5. CO_2 TPD spectra following the elevated pressure CO–O_2 reaction. T = 500 K; (A) Cu(100); P_T = 10 Torr; O_2/CO = 1/25. (B) $Cu_{1.75\ ML}$/Rh(100); P_{CO} = 8 Torr; P_{O_2} = 2.5 Torr. (C) $Cu_{1.75\ ML}$/Rh(100); P_{CO} = 8 Torr; P_{O_2} = 25 Torr. (D) $Cu_{1.75\ ML}$/Rh(100); P_{CO} = 8 Torr; P_{O_2} = 250 Torr. (E) Rh(100); P_{CO} = 8 Torr; P_{O_2} = 250 Torr.

with several Cu coverages, TPD experiments were carried out to monitor the decomposition of the surface carbonate species. Post-reaction CO_2 TPD spectra for several selected reaction conditions are shown in Fig. 5. For comparison, a CO_2 TPD spectrum from Cu-free Rh(100) is also displayed. On Cu-free Rh(100) at low oxygen pressures, no CO_2 desorption was apparent following reaction; however, under oxidizing reaction conditions (P_{O_2} > 50 Torr) the formation of surface carbonate was evident. On the Cu/Rh(100) catalysts, surface carbonates of Cu and Rh were formed.

3. *CO Pressure Dependence*

The CO + O_2 reaction at near stoichiometric conditions on transition metal surfaces, in general, is negative first order in CO partial pressure (6, 10). The CO pressure dependence of CO oxidation on a series of Cu/Rh(100) catalysts was studied at 500 K with copper coverages of 0.00, 0.4, 0.8, 1.0, and 1.6 ML at a constant oxygen pressure of 8 Torr in the CO pressure range 2–50 Torr. The results are summarized in Fig. 6. For the various Cu coverages studied, two distinct CO pressure regions were apparent. In the low pressure regime ($2 < P_{CO} < 15$ Torr) the CO pressure dependence varied between −0.5 and −1. In the high pressure region ($P_{CO} > 15$ Torr) a much less negative, near zero order, CO pressure dependence was observed. In agreement with the results from earlier studies (10), the Cu-free Rh(100) surface exhibited a negative first order CO pressure dependence in the range $2 < P_{CO} < 15$ Torr. At $P_{CO} > 15$ Torr the negative order CO pressure dependence was much less pronounced, i.e., −0.30, however, a small coverage of Cu on Rh(100) (0.4 ML) significantly increased the order. In the low CO pressure range a −0.8-order CO pressure dependence was observed for $Cu_{0.4\ ML}$/Rh(100). As for Cu-free Rh(100), the order in CO pressure was significantly more positive in the high P_{CO} range ($P_{CO} > 15$ Torr). At copper coverages >0.5 ML an approximately −0.5-order CO pressure dependence was observed at $P_{CO} < 15$ Torr and approximately zero order at $P_{CP} > 15$ Torr.

DISCUSSION

The activities shown in Arrhenius form in Fig. 1 indicate that the deposition of Cu onto Rh(100) alters very little the apparent activation energies. The reaction of CO oxidation has been shown to proceed on transition metal surfaces via a Langmuir–Hinshelwood mechanism through the interaction of adsorbed CO and O (6, 9, 10). Under near stoichiometric reaction conditions there is competition between CO and O_2 for free adsorption sites. Except for high temperatures or high O_2/CO ratios, the surface is covered with CO, thus the oxygen adsorption rate is determined by the rate of CO desorption.

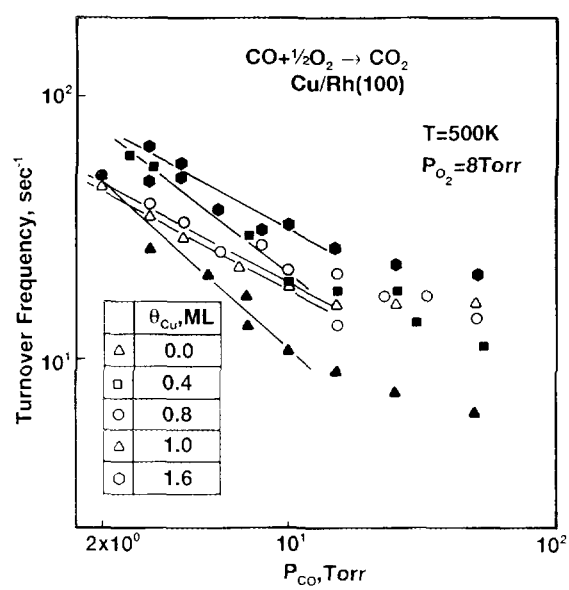

FIG. 6. CO_2 production rate as a function of CO partial pressure on various Cu/Rh(100) catalysts. P_{O_2} = 8 Torr; T = 500 K.

In agreement with our previous work (25), the data of Fig. 1 indicate that deposition of Cu onto Rh(100) enhances its ability to catalyze CO oxidation. Although the catalytic activity is enhanced by the addition of Cu, the apparent activation energy is virtually unchanged on the Cu-covered surfaces. The focus of this work is the role of copper in enhancing the catalytic activity of Rh(100) in CO oxidation.

Recent work has demonstrated that electronic interactions between metals at mixed-metal interfaces define, to a large extent, their chemical properties (24). This interaction, which can be visualized as charge transfer from the electron-rich metal toward the electron-poor metal, alters significantly the adsorptive and catalytic properties of these bimetallic systems (24). For example, for a $Cu_{1.0\ ML}$/Rh(100) bimetallic system the desorption peak temperature of CO is approximately 90 K higher than that for Cu(100) (17) due to the electronic interaction between the Cu adlayer and the Rh(100) substrate. The charge donation from Rh to Cu results in a partially negatively charged Cu, which, in turn, leads to a stronger Cu–CO bond. An increase in the CO adsorption energy for $Cu_{1.0\ ML}$/Rh(100) compared to Cu(100) should lead to an enhanced rate on the mixed-metal catalyst, given the intrinsic weak CO–Cu interaction on Cu(100). On the other hand, we have shown (25) that in the CO oxidation reaction on Cu/Rh(100), Cu is not stable but rather forms 3D Cu_xO agglomerates. The more oxidizing the reactant gas mixture, the faster these agglomerates are formed. Since the apparent activation energy for CO oxidation is greatly influenced by the CO desorption energy, it is anticipated that the apparent activation energy will change significantly from Cu-free Rh(100) to Cu/Rh(100) catalysts. However upon deposition of Cu, the apparent activation energy for CO oxidation is not significantly modified.

The picture that emerges is one in which CO oxidation on Cu/Rh(100) catalysts proceeds in similar fashion to Rh(100). Cu in interacting with the CO + O_2 reactant gas mixture, forms 3D clusters freeing Rh sites for reaction. These Cu-free Rh sites, in turn, are covered predominantly by CO(a). Similar activation energies observed for Rh(100) and Cu/Rh(100) are consistent with the reaction taking place on Rh sites rather than on the Cu/Cu_xO clusters or mixed-metal sites. The Cu/Cu_xO clusters, on the other hand, readily adsorb oxygen thus providing an enhanced coverage of reactive O(a). This enhanced oxygen coverage is believed to be primarily responsible for the increased activity observed for the Cu/Rh(100) systems compared to Cu-free Rh(100).

Since the CO oxidation rate near stoichiometric conditions is O_2 adsorption limited, it is not surprising to find a positive order in oxygen pressure. The probability of oxygen adsorption has been shown to be first order with respect to the number of free Rh sites (28). Accordingly, the oxygen coverage shows a first-order behavior with respect to the oxygen pressure. This positive first-order oxygen pressure dependence is clearly seen for Rh(100) in Fig. 2. Within a narrow oxygen pressure range, the reaction rate changes from positive to negative order. Concomitant with this roll over of the activity at ~90 Torr, the surface oxygen appears in postreaction Auger analysis. As discussed in detail by Peden *et al.* (18, 19), at high O_2/CO ratios the Rh surface becomes oxidized. On this oxidized Rh surface the formation of a carbonate species has been characterized by postreaction high resolution electron energy loss spectroscopy (HREELS) and TPD analysis (19). On oxidized Rh the reaction proceeds via a distinctly different mechanism compared to reduced Rh. While the rate determining step on reduced Rh is CO adsorption, on oxidized Rh the rate-determining step is the decomposition of surface carbonate. The rate of CO oxidation on these oxidized/carbonate-covered surfaces is lower compared to the rate on the reduced metal.

The deposition of ~0.25 monolayers of Cu on Rh(100) results in an increase in CO oxidation activity and a change in the oxygen pressure dependence. The increased catalytic activity is attributed to the enhanced surface oxygen coverage on Rh promoted by Cu. At a Cu coverage of 0.25 ML, however, there are numerous surface Rh atoms with nonadjacent Cu. Accordingly, two different reaction pathways can be rationalized on the $Cu_{0.25\ ML}$/Rh(100) surface. On Rh sites nonadjacent to Cu, CO oxidation occurs at the rate observed for Rh(100). Rh atoms with adjacent Cu atoms, however, exhibit a different rate for CO oxidation, a rate that is much higher. The $Cu_{0.25\ ML}$/Rh(100) catalyst reaches its maximum activity at P_{O_2} = 50 Torr, some 30 Torr lower than for Cu-free Rh(100). It is noteworthy, however, that the maximum turnover frequencies are identical for both catalysts. The enhanced surface coverage of oxygen on the Cu-promoted Rh(100) leads to oxidation of the Rh surface at a lower oxygen pressure compared to Rh(100). Figure 4 clearly shows that as the activity approaches the maximum, the onset of surface oxidation is apparent. In contrast to the clean Rh(100) surface, where no surface oxygen is evident in post-reaction Auger analysis below the maximum catalytic activity, the $Cu_{0.25\ ML}$/Rh(100) system shows oxygen on the surface even at the lowest oxygen pressure of 2 Torr. This surface oxygen at low oxygen pressures is associated exclusively with Cu. Contrary to the Rh(100) surface, The $Cu_{0.25\ ML}$/Rh(100) surface exhibits a stable activity over a relatively wide range of oxygen pressures. Within this oxygen pressure region the reaction rate is limited by the reaction of CO(a) and O(a). At these high oxygen pressures the surface is covered predominantly by oxygen, that is, the surface coverage of adsorbed CO is low. The maximum reaction rate for CO oxidation has been shown to occur at CO surface coverages of $<1\%$ (9,

12). Under reaction conditions of high O_2/CO ratios (>30) the reaction rate becomes negative order in oxygen pressure. Under these highly oxidizing reaction conditions the rate determining step has been shown to be the decomposition of surface carbonate (18, 19).

The oxygen partial pressure dependence of the CO_2 production rate on Cu/Rh(100) catalysts with Cu coverages higher than 0.5 ML is very similar to that observed on Rh(100). At oxygen partial pressures up to 50 Torr a positive first-order oxygen pressure dependence is seen. Then, over a wide pressure range, the activity is independent of the oxygen pressure. At high oxygen pressures the activity falls for all catalysts. The first-order oxygen pressure dependence is consistent with and supports our proposed reaction mechanism. On these catalysts, contrary to the those with Cu coverages <0.5 ML, one kind of active center is present, i.e., Rh atoms with adjacent Cu atoms. The reaction between adsorbed CO and O takes place on these Rh sites; however, the enhanced oxygen coverage induced by Cu promotes higher rates on Cu/Rh(100) compared to Cu-free Rh(100).

At the lowest oxygen pressures Cu/Rh(100) catalysts with $\theta_{Cu} > 1.0$ ML exhibited activity near that of pure Cu. For example, for the $Cu_{1.75\ ML}$/Rh(100) catalyst the activity at an oxygen pressure of 1.0 Torr is lower than that for Rh(100). These results clearly show the role of Cu clustering. Initially, at Cu coverages >1.0 ML, the Rh(100) substrate is fully covered with Cu and the rate reflects that of pure Cu. However, increasing the oxygen pressure to ~2.5 Torr leads to a significant increase in catalytic activity; above 2.5 Torr oxygen the catalytic behavior corresponds to that observed for submonolayer Cu.

The clustering of the Cu overlayers is clearly evident in the Cu/Rh and O/Rh Auger peak ratios shown in Figs. 3 and 4. The Cu/Rh ratio initially drops in the low O_2 pressure range for $Cu_{1.1\ ML}$/Rh(100) and $Cu_{1.75\ ML}$/Rh(100). The higher Cu coverages exhibit an accelerated decrease in the Cu/Rh Auger ratio, consistent with more rapid clustering of Cu. At relatively low oxygen pressures the kinetics of the clustering is insufficiently slow to significantly alter the Cu morphology. However, with increasing oxygen pressures the Cu clustering process accelerates and the Cu/Rh Auger ratio attenuates accordingly. Concomitantly, the O/Rh ratio decreases reflecting the additional substrate Rh(100) exposed by the Cu clustering. Between ~2.5 and ~25 Torr the Cu morphology is stable and the reaction is positive first order in oxygen pressure. At oxygen pressures >25 Torr, however, the onset of oxidation of the Rh(100) begins with the rate of oxidation being proportional to the initial Cu coverage. The increase in the O/Rh Auger ratio is tracked by the Cu/Rh ratio, a result that can be attributed to either one of two possibilities: (a) as the Rh surface becomes oxidized the Auger electrons originated from the Rh atoms are attenuated by the oxide layer, leading to an increase in the Cu/Rh ratio; or (b) oxidation of the Rh results in "wetting" of the Rh oxide by Cu oxide. The AES results were insufficient to distinguish these possibilities.

The negative first order CO partial pressure dependence for Rh(100) (Fig. 6) is in agreement with previous work (10) and shows the inhibiting role of adsorbed CO on the reaction. It is noteworthy that in the kinetic investigations of Peden *et al.* (10), the maximum CO pressure studied was ~20 Torr. At higher CO pressures, there is a significant deviation from this −1 order in CO partial pressure, even for Rh(100). In a wide range of CO pressures about stoichiometry, the Rh(100) surface is covered primarily by CO; at relatively high CO pressures, the CO coverage saturates and the inhibiting effect of CO on the reaction becomes less pronounced.

The presence of Cu on Rh(100) does not affect dramatically the CO pressure dependence of CO_2 production. At a Cu coverage of 0.4 ML, the CO pressure dependence is less negative than for Rh(100); at higher CO pressures the rate is almost independent of CO pressure. At Cu coverages greater than 0.5 ML, within the low CO pressure region, the reaction is −0.5 order in CO pressure and essentially independent of the Cu coverage. On surfaces with high initial Cu coverages and at relatively high CO pressures, (>15 Torr) the reaction is approximately zero order in CO pressure. The approximate −0.8 order for the $Cu_{0.4\ ML}$/Rh(100) sample can be rationalized using our model with two active sites. On the Rh sites with no adjacent Cu, the reaction exhibits −1.0 order in CO pressure, characteristic of Rh(100). For Rh sites with adjacent Cu, however, because of the enhanced adsorption of oxygen, the reaction order is −0.5.

On supported Cu/Pd bimetallic catalysts, Choi and Vannice (26), have measured the order of reaction with respect to CO. At low CO pressures the order of reaction is negative, as observed for a pure Pd catalyst. At higher CO pressures, however, the CO pressure dependence shifts to positive order, characteristic of a pure Cu catalyst. At these high CO pressures the reaction on the Cu/Pd catalyst takes place almost exclusively on the Cu sites. It should be noted, however, that Cu and Pd readily form an alloy, whereas Cu and Rh, under the conditions of these experiments, do not. Thus, the Cu in the Cu/Pd catalysts is uniformly distributed throughout the Pd particles, while the Cu in the Cu/Rh(100) catalyst forms 3D Cu_xO clusters.

CONCLUSIONS

1. The rate of CO oxidation is higher on Cu/Rh(100) catalysts compared to pure Cu or pure Rh catalysts. The similarities in the apparent activation energies observed

for Rh(100) and Cu/Rh(100) catalyst suggest a common reaction mechanism.

2. On the Cu/Rh(100) catalysts the oxygen and CO pressure dependencies are characteristic of Rh(100). At $\theta_{Cu} < 0.5$ ML, a dual mechanism is operative. On Rh sites with nonadjacent Cu, CO oxidation occurs just as for Rh(100). Rh sites with adjacent Cu exhibit enhanced reactivity toward CO oxidation due to the Cu-induced higher oxygen coverages.

3. For oxidized Cu/Rh catalysts under reaction conditions, Cu- and Rh-carbonates are formed.

ACKNOWLEDGMENT

We acknowledge with pleasure the support of this work by the Department of Energy, Office of Basic Sciences, Division of Chemical Sciences, and the Robert A. Welch Foundation.

REFERENCES

1. Cant, N. W., Hicks, P. C., and Lennon, B. S., *J. Catal.* **54,** 372 (1978).
2. Cant, N. W., and Angove, D. E., *J. Catal.* **97,** 36 (1986).
3. Oh, S. H., and Carpenter, J. E., *J. Catal.* **80,** 472 (1983).
4. Schlatter, J. C., and Taylor, K. C., *J. Catal.* **49,** 42 (1977).
5. Choi, K. I., and Vannice, M. A., *J. Catal.* **131,** 1 (1991).
6. Engel, T., and Ertl, G., *Adv. Catal.* **28,** 1 (1979).
7. (a) Bonzel, H. P., and Ku, R. J., *J. Phys. Chem.* **59,** 205 (1973); (b) Bonzel, H. P., and Burton, J. J., *Surf. Sci.* **52,** 223 (1975); (c) Palmer, R. L., and Smith, J. N., *J. Chem. Phys.* **60,** 1453 (1974); (d) Gland, J. L., and Kollin, E. B., *J. Chem. Phys.* **78**(2) 963 (1983).
8. Berlowitz, P. J., Peden, C. H. F., and Goodman, D. W., *J. Phys. Chem.* **90,** 5213 (1988).
9. Schwartz, S. B., Schmidt, L. D., and Fisher, G. B., *J. Phys. Chem.* **90,** 6194 (1986).
10. Peden, C. H. F., Goodman, D. W., Blair, D. S., Berlowitz, P. J., Fisher, G. B., and Oh, S. H., *J. Phys. Chem.* **92,** 1563 (1988).
11. Goodman, D. W., and Peden, C. H. F., *J. Phys. Chem.* **90,** 4839 (1986).
12. Leung, L-W. H., and Goodman, D. W., *Catal. Lett.* **5,** 353 (1991).
13. Daniel, W. M., and White, J. M., *Int. J. Chem. Kinet.* **17,** 413 (1985).
14. Peden, C. H. F., and Hoffmann, F. M., *Catal. Lett.* **10,** 91 (1991).
15. Hoffmann, F. M., Weisel, D. M., and Peden, C. H. F., *Surf. Sci.* **253,** 59 (1991).
16. Campbell, C. T., and White, J. M., *J. Catal.* **54,** 289 (1978).
17. Jiang, X., and Goodman, D. W., *Surf. Sci.* **255,** 1 (1991).
18. Peden, C. H. F., Berlowitz, P. J., and Goodman, D. W., *in* "Proceedings, 9th International Congress on Catalysis, Calgary, 1988" (M. J. Phillips and M. Ternan, Eds.), p. 1214. Chemical Institute of Canada, Ottawa, 1988.
19. Peden, C. H. F., and Houston, J. E., *J. Catal.***128,** 405 (1991).
20. Oh, S. H., Fisher, G. B., Carpenter, J. E., and Goodman, D. W., *J. Catal.* **100,** 360 (1986).
21. Bowker, M., Guo, Q., and Joyner, R., *Surf. Sci.* **253,** 33 (1991).
22. Campbell, C. T., *Annu. Rev. Phys. Chem.* **41,** 775 (1990).
23. Goodman, D. W., and Peden, C. H. F., *J. Chem. Soc. Faraday Trans. 1* **83,** 1967 (1987).
24. (a) Rodriguez, J. A., and Goodman, D. W., *J. Phys. Chem.* **95,** 4196 (1991); (b) Campbell, R. A., Ph.D. Thesis, Texas A&M University, 1992.
25. Szanyi, J., and Goodman, D. W., *Catal. Lett.* **14,** 27 (1992).
26. (a) Choi, K. I., and Vannice, A. M., *J. Catal.* **131,** 22 (1991); (b) **131,** 36 (1991).
27. Szanyi, J., and Goodman, D. W., *Rev. Sci. Instr.* **64,** 2350 (1993).
28. Yates, J. T., Thiel, P. A., and Weinberg, W. H., *Surf. Sci.* **82,** 45 (1979).
29. Szanyi, J., and Goodman, D. W., submitted for publication.
30. Imelik, B., Naccache, C., Coudurier, G., Praliaud, H., Meriaudeau, P., Gallezot, P., Martin, G. A., and Vedrine, J. C. (Eds.), "Metal–Support and Metal–Additive Effects in Catalysts." Elsevier, Amsterdam, 1982.
31. Sinfelt, J. H., "Bimetallic Catalysts: Discoveries, Concepts and Applications." Wiley, New York, 1983.